

The Influence of Parameters on the Flow Structure in Semidetached Binary Systems: 3D Numerical Simulation

D.V.Bisikalo¹

Institute of Astronomy of the Russian Acad. of Sci., Moscow, Russia

A.A.Boyarchuk

Institute of Astronomy of the Russian Acad. of Sci., Moscow, Russia

O.A.Kuznetsov²

Keldysh Institute of Applied Mathematics, Moscow, Russia

V.M.Chechetkin

Keldysh Institute of Applied Mathematics, Moscow, Russia

ABSTRACT

The basic parameters determining the flow pattern for a nonviscous, non-heat-conducting gas in a semidetached binary system without a magnetic field are identified. Three-dimensional gas-dynamical modeling of the mass transfer enables investigation of the influence of these parameters on the structure of gas flows. The parameter on which the flow pattern depends most strongly is the adiabatic index γ . The effect of other parameters is small, and only leads to unimportant quantitative changes in the solutions obtained. The main properties of flows typical of semidetached binaries without magnetic fields are summarized.

¹E-mail address: *bisikalo@inasan.rssi.ru*

²E-mail address: *kuznecov@spp.keldysh.ru*

1. Introduction

Semidetached binary systems belong to the class of interacting stars, in which one of the components fills its Roche lobe and there is mass exchange between the components through the inner Lagrange point. Beginning with the pioneering work of Prendergast [1], the gas dynamics of matter flows in semidetached systems have been extensively investigated by many authors. As a rule, two-dimensional (2D) numerical models have been used in calculations (see, for example, [2–9]). Unfortunately, the limitations of the 2D approach cast doubt on the adequacy of some results obtained using these models. Analytical studies of the applicability of 2D models for accretion disks [10] have shown that these models give correct results only in certain limited cases (with an adiabatic index $\gamma = 1$ for disks in an external gravitational field and $\gamma = 2$ for self-gravitating disks). In all other cases, a three-dimensional (3D) treatment must be employed. The comparison [11] of numerical calculations performed using 2D and 3D models confirmed the limited applicability of 2D models, and demonstrated the necessity of using 3D models in numerical analyses of the flow structures in semidetached binaries.

Three-dimensional modeling calls for substantial computational resources, and for this reason, such studies are few in number (the best known are [12–21]). In addition, the morphology of the flows in semidetached binaries is examined in only a few of these, since many of these studies were performed in a restricted formulation in which the process of establishment of flow formation was not taken into consideration. The variety of binary systems studied and approaches used makes it impossible to generalize the results obtained, or to make at least qualitative predictions about the flow structures expected for semidetached systems. At the same time, such studies are extremely important, since data on the structure of gas flows are necessary for interpretation of the observational data, and the time-consuming nature of 3D modeling makes it impossible to compute the flow pattern for each particular system.

Here, we consider the results of 3D numerical modeling of the flow of an ideal gas in a semidetached binary system assuming the absence of magnetic field and radiative heating and cooling of the gas. To make the study more systematic, we generalize the results of eight of our own calculations, and have also used, in some cases, the results of other studies. We identified

the basic parameters of this problem (Section 2) and successively examined the effect of each parameter on the flow structure (Section 3). Features of the flow brought about by the influence of various parameters and the typical characteristics of the flow structure are described in Section 4.

2. Parameters of the Problem

In order to perform gas–dynamical studies of the flow structures in binary systems, it is necessary to specify values of the parameters describing the system under consideration and of the parameters used in the mathematical model used.

2.1. Parameters of binary system

Numerical analyses of the matter flows in binary systems to not require the specification of all seven orbital elements for the binary star, since the orbital plane is assumed to be known in advance. In this case, we can describe the motion of the system’s components using the mass of the donor star M_1 and the mass of the accretor star M_2 (or equivalently, the total mass of the system M and the mass ratio of the components $q = M_2/M_1$), the semimajor axis of the orbit A , the rotation period P_{orb} (or, equivalently, the angular velocity $\Omega = 2\pi/P_{orb}$), and the orbital eccentricity e . Note that the application of Kepler’s third law decreases the required number of parameters, making it possible to use, instead of the four parameters M , q , A , and Ω , any three of these to describe the system in a point-mass approximation. The geometric sizes of the components should also be included among the parameters describing the system. For the semidetached systems considered here, we assume that the donor star fills its Roche lobe and, therefore, its geometric characteristics are completely specified by the parameters of the system. The size of the accretor star R_2 is an independent parameter that must be given separately.

2.2. Model parameters

In our numerical model, we use the Euler equations in the form of integral conservation laws to describe the flow of a nonviscous, non-heat-conducting gas in a binary system without magnetic or radiation fields. This permits us to obtain discontinuous (non-isentropic) solutions satisfying the Rankine–Hugoniot conditions at the discontinuities (shock waves and contact discontinuities). We complete the system of

gas–dynamical equations with the equation of state of an ideal gas with adiabatic index γ : $P = (\gamma - 1)\rho\varepsilon$, where P is the pressure, ρ is the density, and ε is the specific internal energy.

To solve the system of gas–dynamical equations, we must specify the boundary conditions at the surfaces of the system’s components and at the surface of the computation region. The states of the gas in the near-surface layers of the donor and accretor stars are determined by the gas densities ρ_1 and ρ_2 , the temperatures T_1 and T_2 (or, equivalently, the sound speeds c_1 and c_2), and the gas-velocity vectors \mathbf{v}_1 and \mathbf{v}_2 . The boundary conditions at the stellar surfaces are obtained by the standard procedure of solving Riemann problem between the states immediately under the stellar surface and the first computation node (see, for example, [2, 3]). A free-outflow condition is specified at the outer boundary of the computation region.

Thus, in our formulation, the motion of a nonviscous gas in a binary system without magnetic and radiation fields depends on five parameters specifying the binary system: q , A , Ω , e , R_2 and seven model parameters: γ , ρ_1 , c_1 , \mathbf{v}_1 , ρ_2 , c_2 , \mathbf{v}_2 .

Understanding the necessity of studying successively the roles of individual parameters, we introduce a number of additional constraints that decrease the total number of parameters. In particular, we assume that we can neglect the stellar wind produced by the accretor star. This is standard in studies of flows in semidetached binaries, and is widely used in computations (see, for example, [12–19]). In this case, the only influence of the accretor on the flow of matter is gravitational, and we can adopt a condition of complete accretion at its surface, i.e., the condition that all gas reaching the surface of this component is absorbed. In order to be able to perform a stage-by-stage investigation of the effect of various parameters on the flow structure, we also add a number of constraints on the type of system under consideration: we assume that (i) the orbits of the components are circular, which allows us to fix the parameter $e = 0$; (ii) the accretor is a compact object (a white dwarf, neutron star, or black hole), so that, when $R_2 \ll A$, the general structure of the flow is determined only by the gravitational field of the accretor and, accordingly, the parameter R_2 can be excluded; (iii) the rotation of the donor star is synchronized with the orbital motion of the system, so that, in a reference frame rotating with the angular velocity of the system, the gas velocity at the surface

of the donor star is directed along the normal to this surface, and we can replace the vector parameter \mathbf{v}_1 by the scalar parameter v_1 (equal to the velocity component perpendicular to the donor-star surface).

In the above formulation, the flow structure in the binary system depends on seven parameters: q , A , Ω , γ , ρ_1 , c_1 , v_1 . It is noteworthy that the solution is not affected by the boundary density at the donor star, since the system of equations can be scaled with respect to ρ (and simultaneously with respect to the pressure P). In the numerical model, an arbitrary ρ_{ho1} value can be used. When considering a specific system with known mass-loss rate, however, we must scale the calculated density values by the ratio of the true and model densities at the surface of the donor star if we wish to find the real density values for the system. For convenience in the numerical solution, the original system of equations can be written in dimensionless form. Following the usual practice (see, for example, [2, 3]), we use the distance A between the components and the reciprocal of the angular rotation velocity of the system Ω^{-1} , to make the equations dimensionless with respect to space and time, respectively. In this case, the remaining six parameters determining the flow structure can be reduced to a combination of four dimensionless parameters $q = M_2/M_1$, $\epsilon = c_1/(\Omega A)$, $\mathcal{M} = v_1/c_1$, γ , and solutions obtained for two systems with the same parameter values will differ only by a scaling factor.

3. Results

To determine the influence of various parameters on the flow structure, we carried out 3D numerical modeling of several binary systems. We successively varied each of the parameters while fixing the values of the remaining parameters. It is evident that in a full analysis, the number of values considered for each parameter (in the total characteristic range of values) must be as large as possible. Unfortunately, 3D modeling requires substantial computational resources, and we restricted ourselves to only eight calculations. The parameters used in these calculations are summarized in Table I. The limited number of calculations makes it impossible to study the dependence of the results on a selected parameter in detail. Nevertheless, analysis of our results enables identification of the parameters most strongly affecting the flow structure, and determination at a qualitative level of trends in the solution behavior.

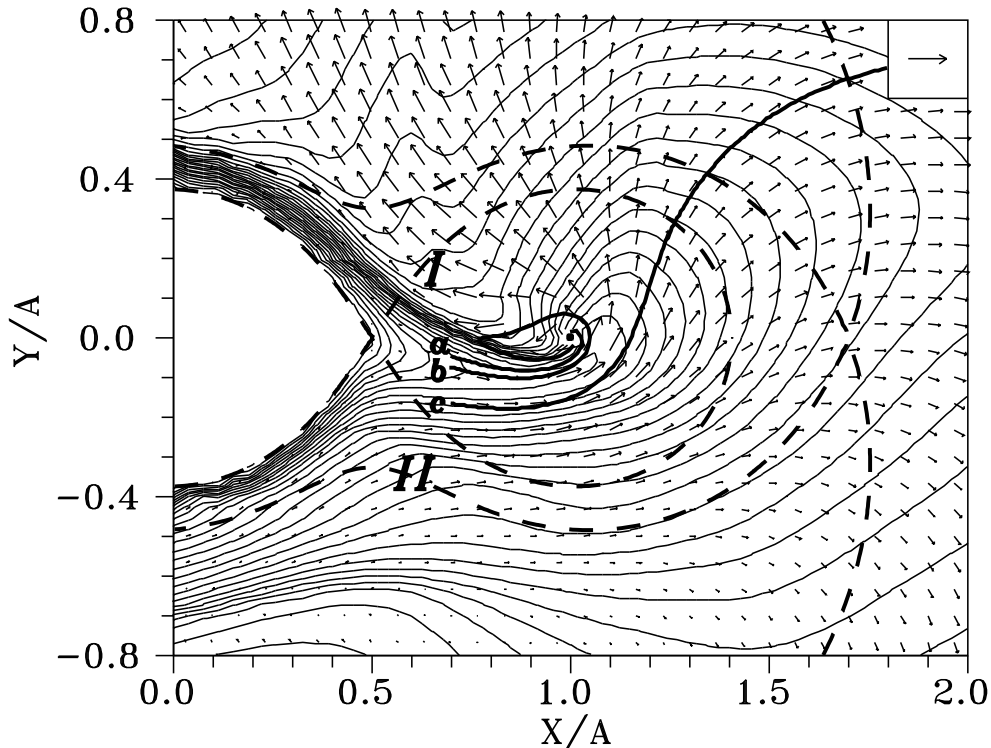


Fig. 1.— (a) density contours and velocity vectors in the equatorial plane of the binary system for calculation 1 specified in Table I. The vector in the upper right corner corresponds to the velocity $4A \cdot \Omega$. Three flowlines, denoted ‘a’, ‘b’, and ‘c’ illustrate the directions of the flow of matter in the system. The dashed lines are the Roche equipotential surfaces.

Taking into account the computer-intensive nature of the problem, we included our previous results [22–25] in our analysis. Additional computations were made in three cases (computations 3, 4, 5 in Table I), in order to fill out the field of parameter values. We also used results presented by other authors when their parameters differed from those in Table I.

The computation results for each of the eight cases presented in Table I are given in Figures 1–8. The upper panels (Figures 1a–8a) depict density contours and velocity vectors in the equatorial plane of the system illustrating the morphology of gas flows in the system. A vector showing the velocity scale is given in the upper right corner of each plot. In all cases, the length of this vector corresponds to the velocity $4A \cdot \Omega$. We also show in the figures three flowlines marked by letters ‘a’, ‘b’, and ‘c’, which illustrate the directions of the flow of matter in the system. Density contours and velocity vectors in the plane passing through the

Table I.

Case N	q	ϵ	\mathcal{M}	γ
1	1	0.15	0.083	1.2
2	1	0.15	0.083	1.01
3	1	0.016	0.083	1.2
4	1	0.016	0.083	1.01
5	1	0.016	1	1.01
6	5	0.016	0	1.01
7	5	0.016	1	1.01
8	5	0.04	1	1.01

accretor and perpendicular to the line connecting the centers of the two components are shown in the lower panels (Figures 1b–8b). The velocity scale is specified by the vector in the upper right corner of these panels, which corresponds to the velocity $2A \cdot \Omega$. For convenience, the range of density variation in Figures 1b–

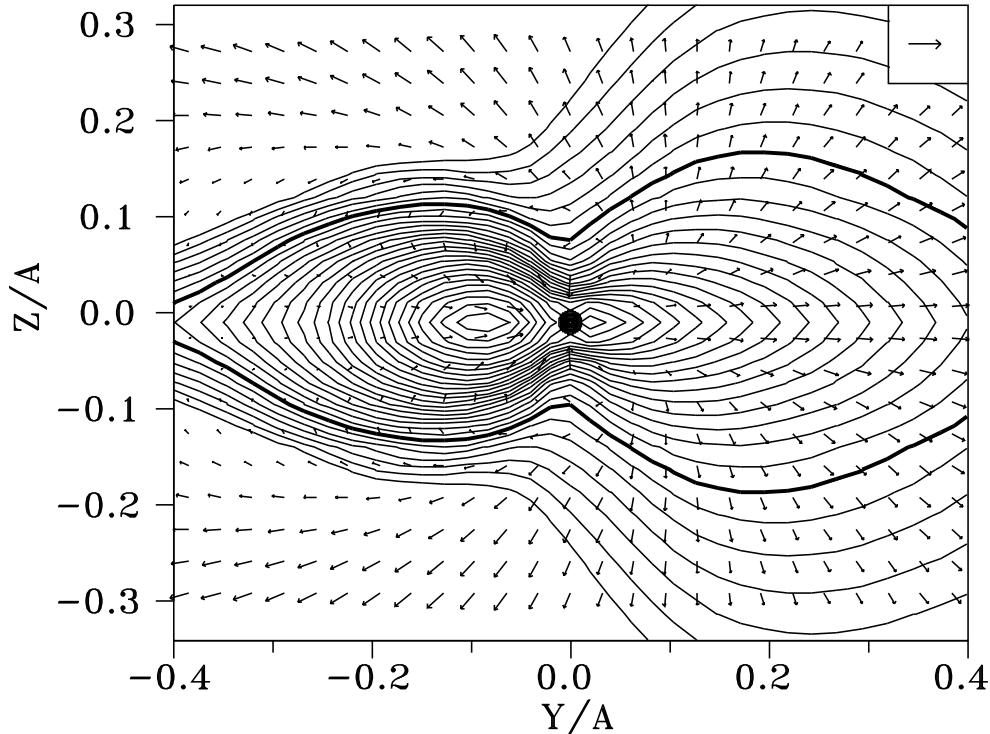


Fig. 1 – *continued*.— (b) density contours and velocity vectors in the plane passing through the accretor star and perpendicular to the line connecting the centers of the system’s components. The vector in the upper right corner corresponds to the velocity $2A \cdot \Omega$. The range of the density variations is $0.1 - 0.0003\rho_0$. The thick solid line corresponds to the density $0.001\rho_0$.

8b is chosen to be the same, and to be equal to $0.1 - 0.0003\rho_0$. The thick line corresponds to the density $0.001\rho_0$. The flow pattern in the figures is stationary and corresponds to a steady-state flow regime.

Analysis of the results presented in this paper enables investigation of the influence of various parameters on the flow structures in semidetached binary systems.

3.1. The effect of γ

The dependence of the flow pattern on the adopted value of the parameter γ can be established by comparing the results of calculations in cases 1 and 2, and in cases 3 and 4. We varied only the parameter γ in these pairs of cases, with all other parameters having fixed values.

Analysis of the results presented in the figures shows that, in the quasi-stationary case ($0.001\rho_0$), the flow pattern is characterized by the presence of an accretion disk and circumbinary envelope (Fig-

ures 2 and 4). The details of the flow structure in the cases under consideration are largely determined by the presence of the circumbinary envelope, and were considered by us in [22–25]. Below, we give only a brief description of the main features of the flow for this case, referring the reader to [22–25] for a more detailed discussion. Analysis of the gas flows allows us to divide the matter in the stream flowing from L_1 into three parts: the first produces a quasi-elliptical accretion disk (flowline ‘a’) and continues to participate in the accretion process, losing angular momentum under the action of viscosity; the second (flowline ‘b’) flows around the accretor outside the disk; the third part of the stream moves toward the Lagrange point L_2 (flowline ‘c’), and a significant portion of this matter changes the direction of its motion under the action of the Coriolis force and remains in the system. The matter remaining in the system and not involved directly in the accretion process (flowlines ‘b’ and ‘c’) forms the circumbinary envelope of the system. A significant portion of the envelope gas

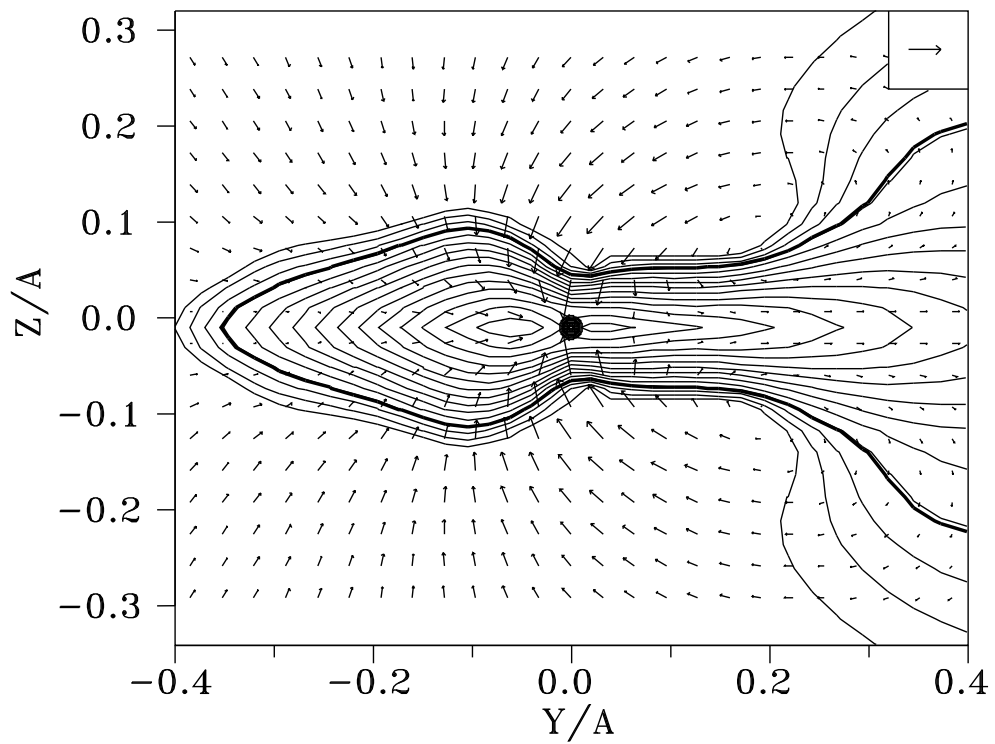
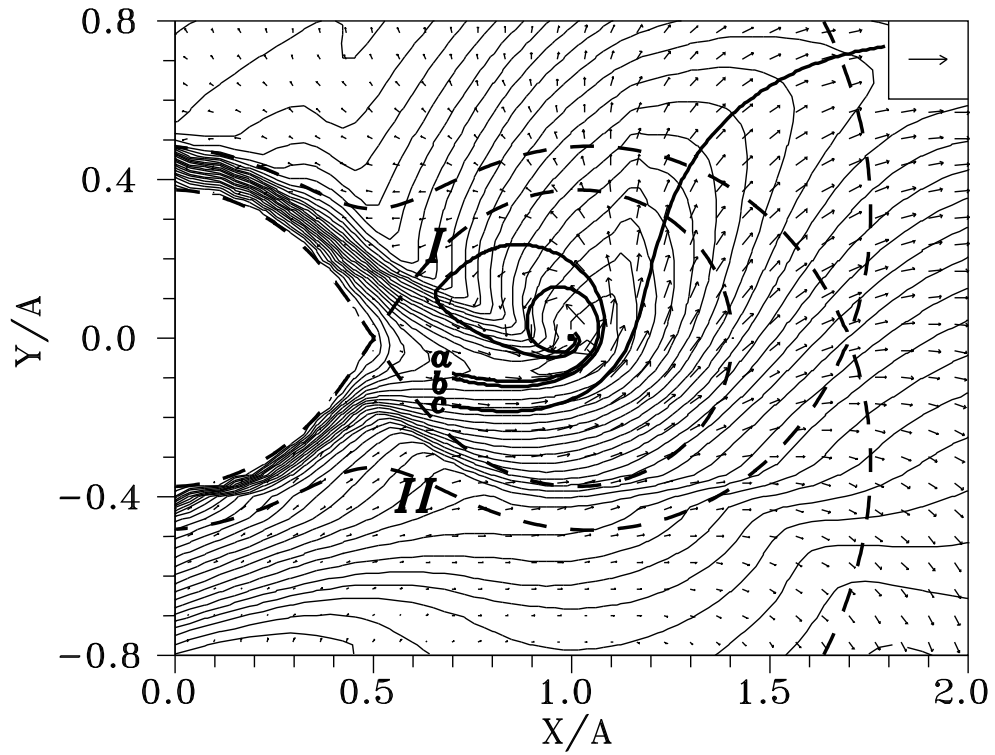


Fig. 2.— Same as Figure 1 for calculation 2 from Table I.

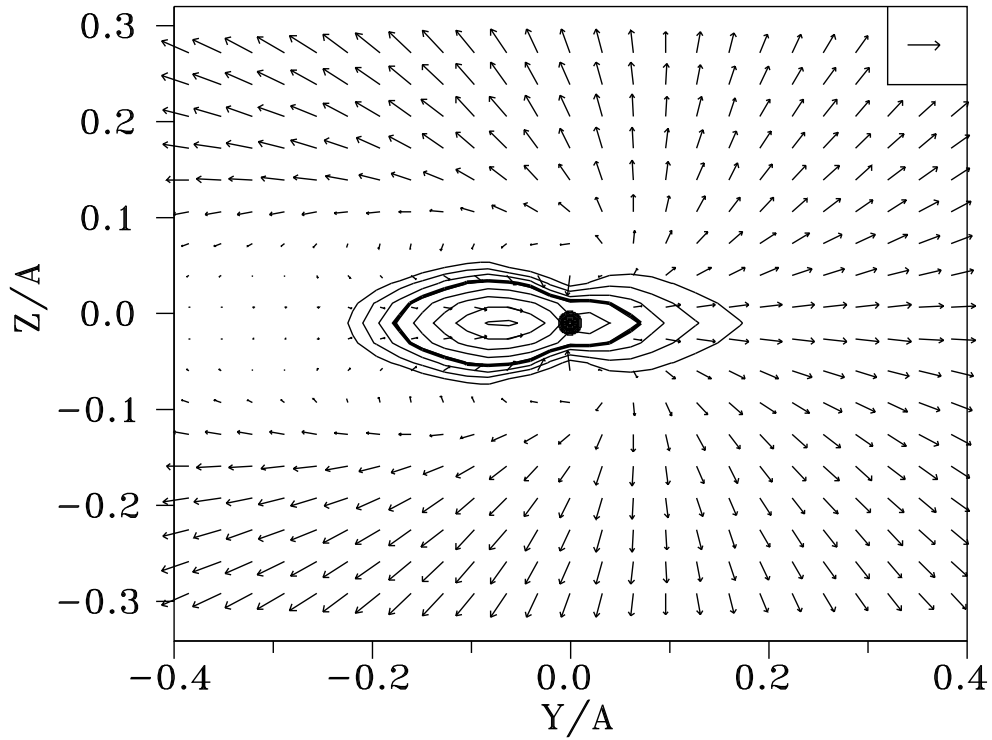
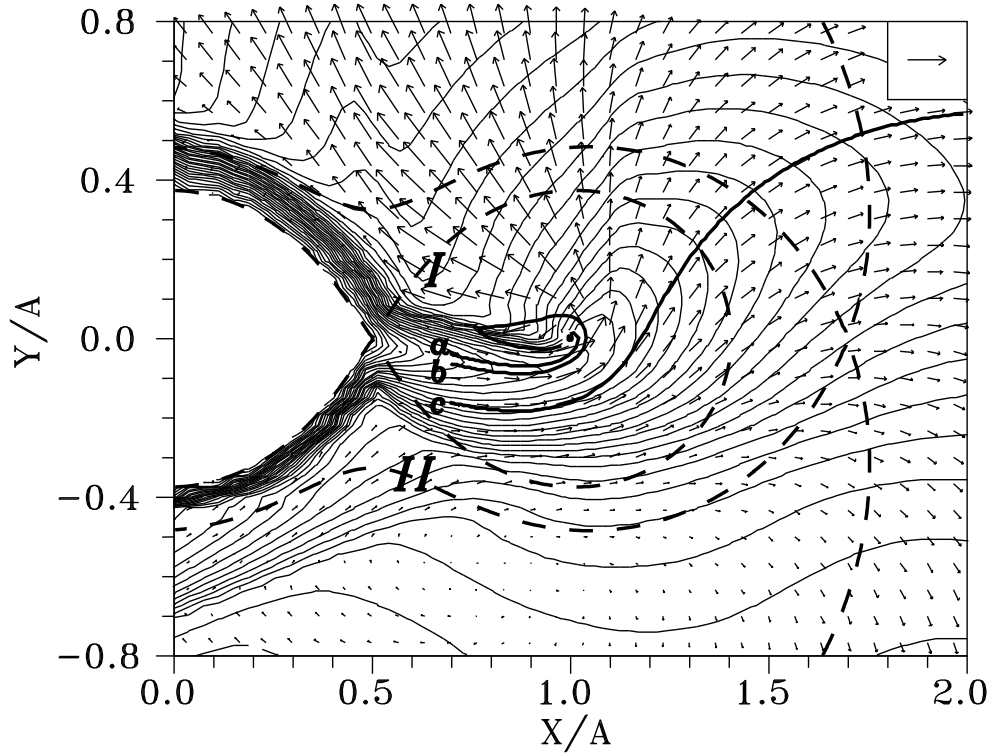


Fig. 3.— Same as Figure 1 for calculation 3 from Table I.

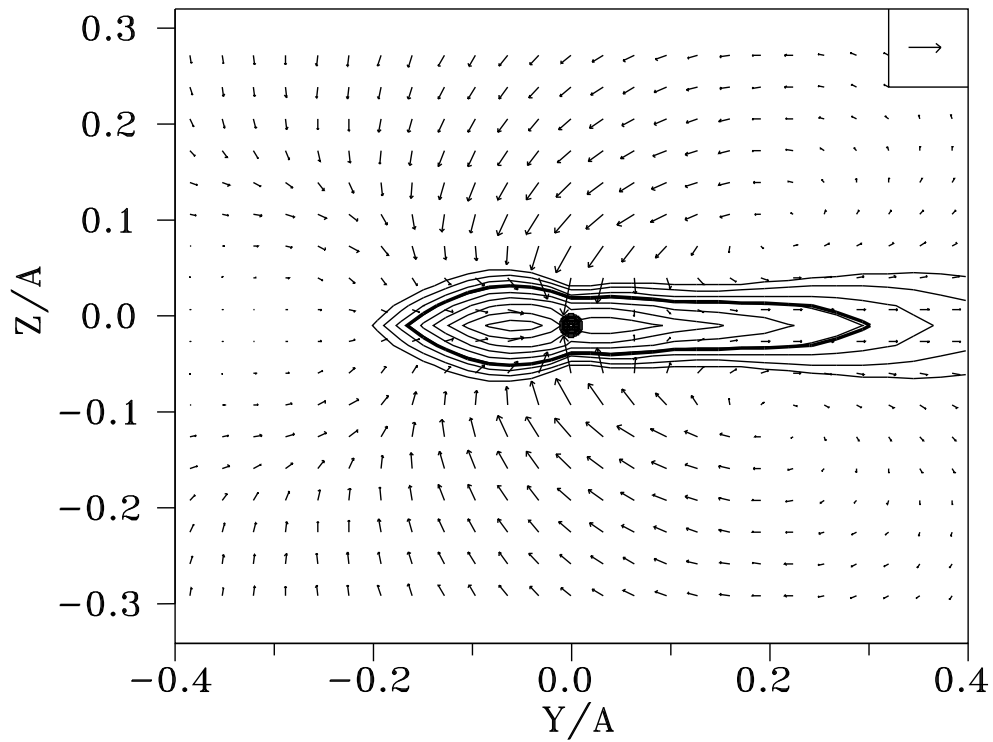
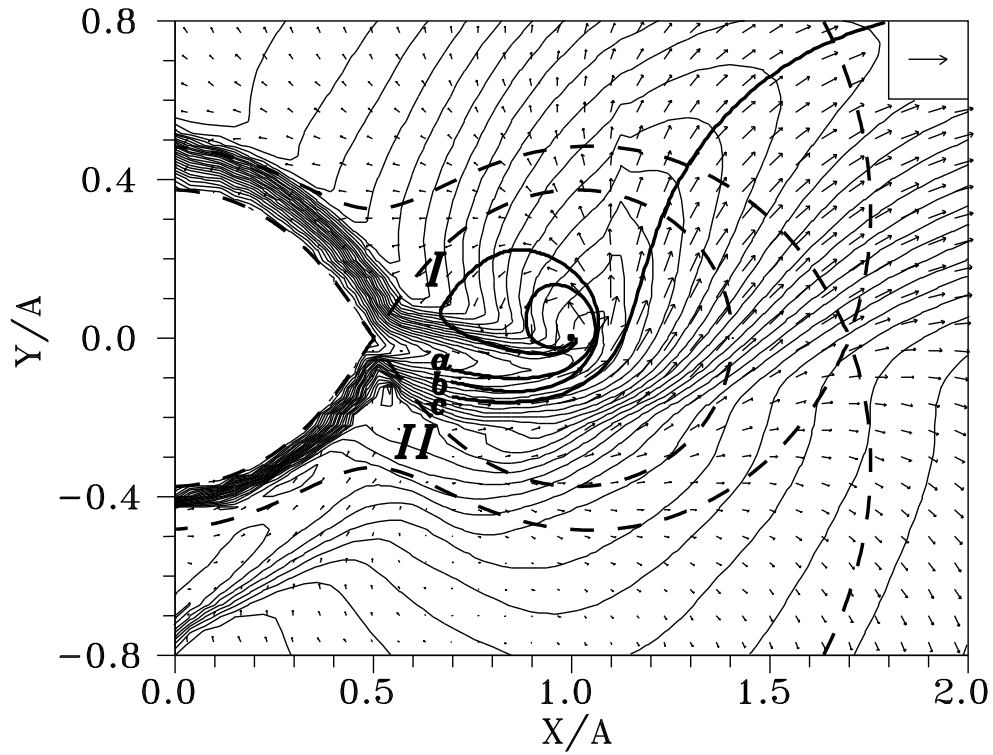


Fig. 4.— Same as Figure 1 for calculation 4 from Table I.

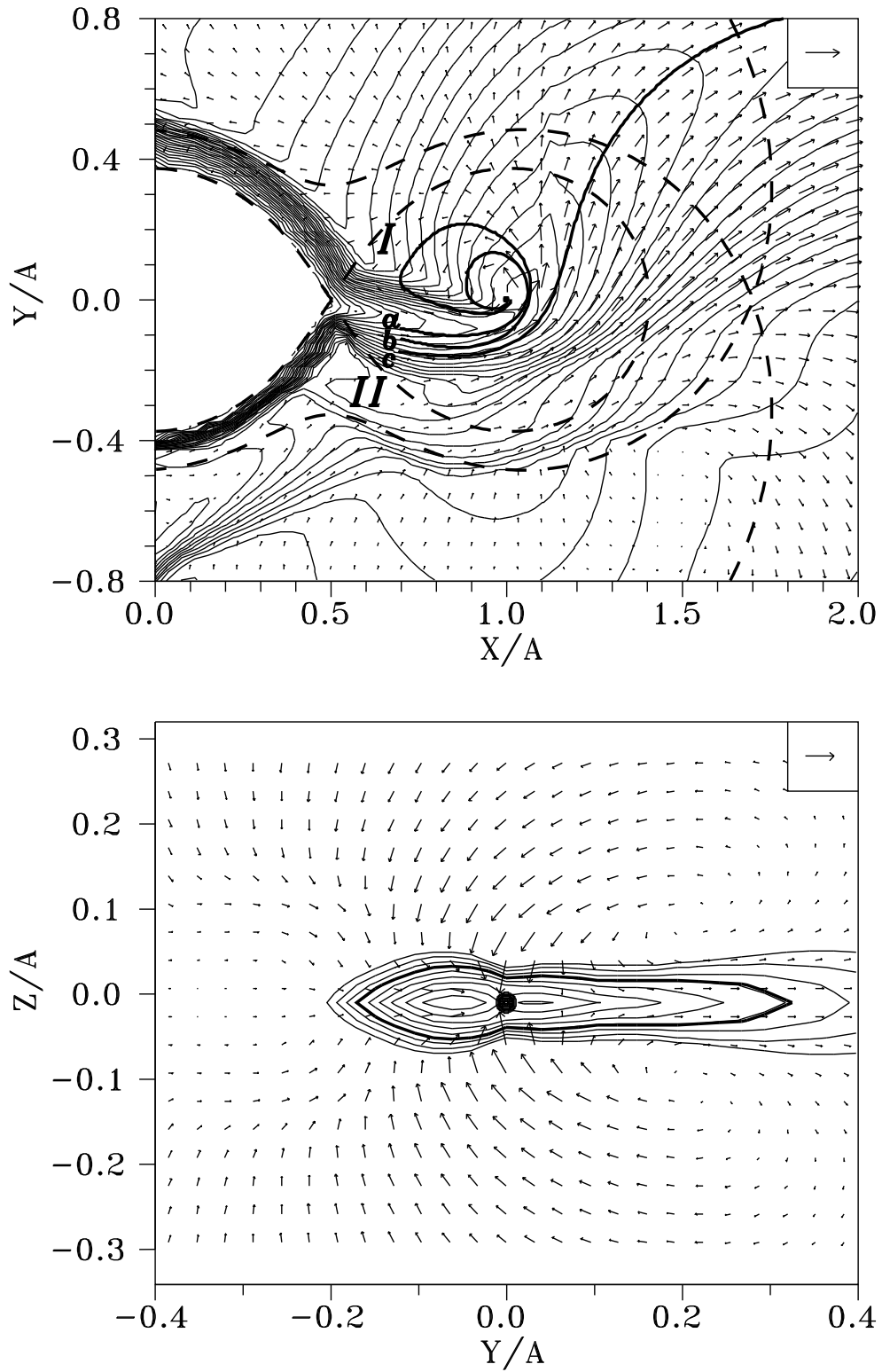


Fig. 5.— Same as Figure 1 for calculation 5 from Table I.

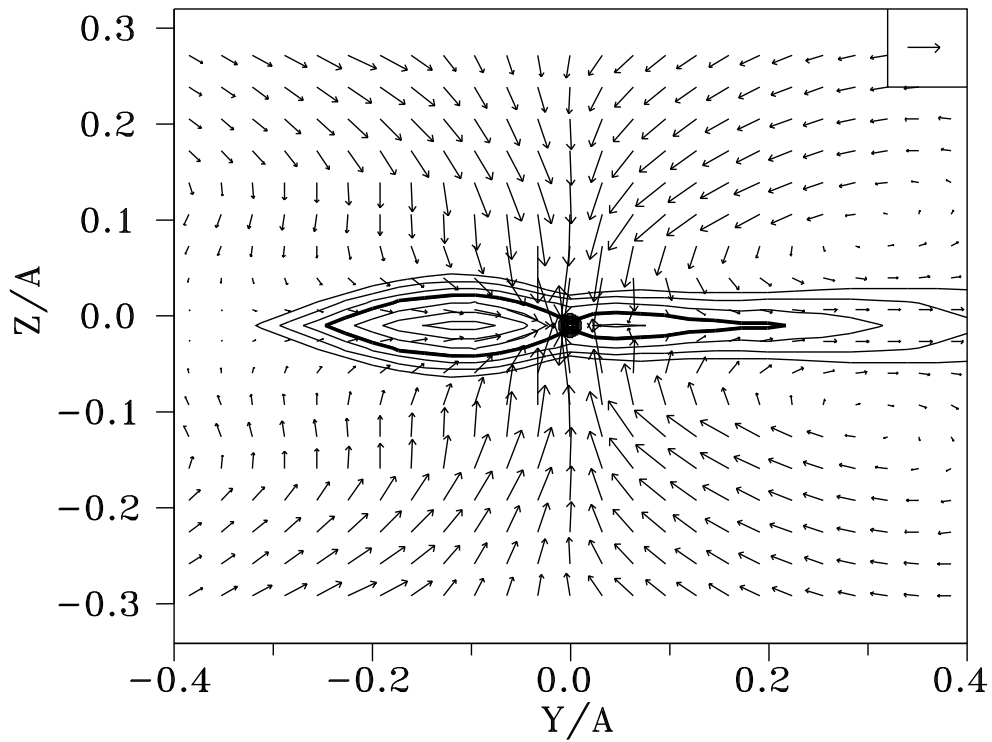
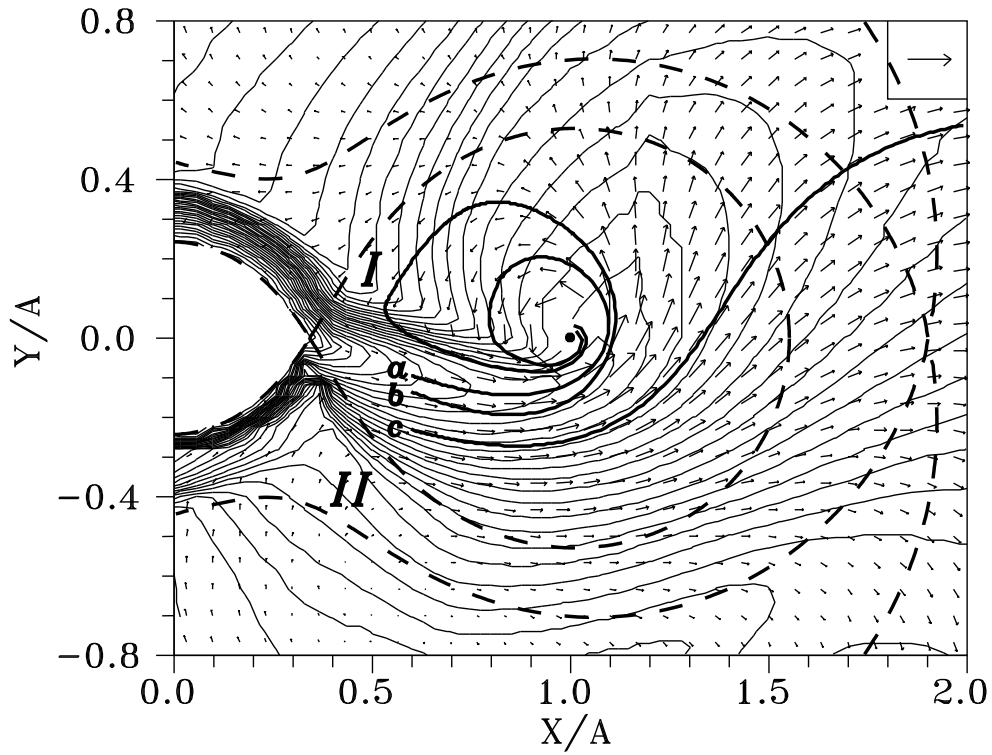


Fig. 6.— Same as Figure 1 for calculation 6 from Table I.

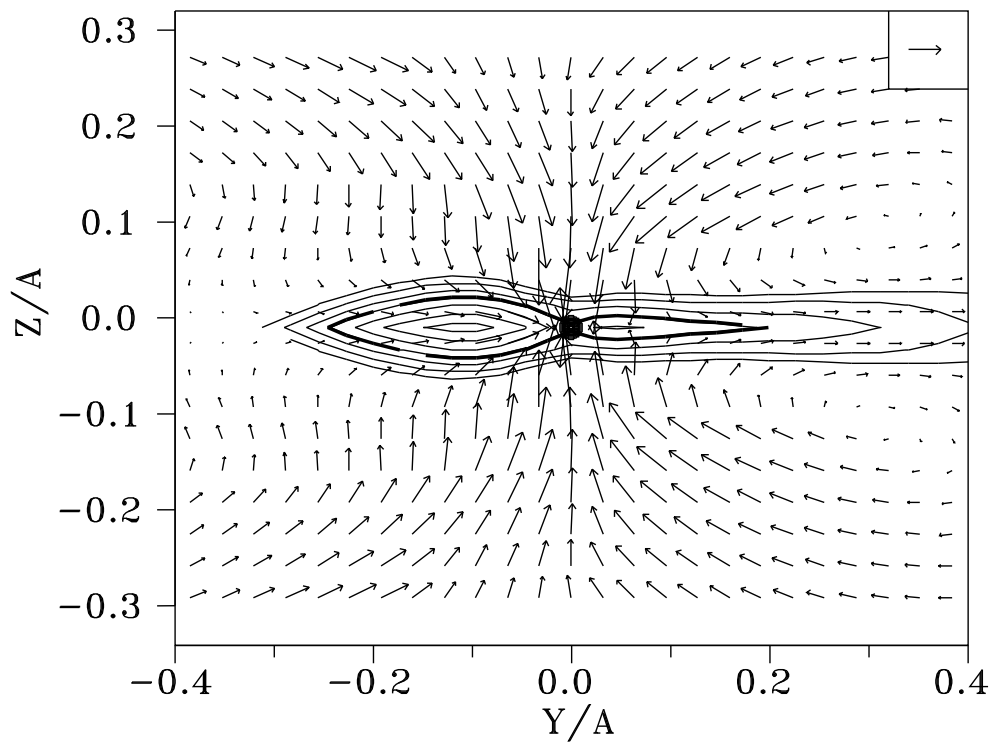
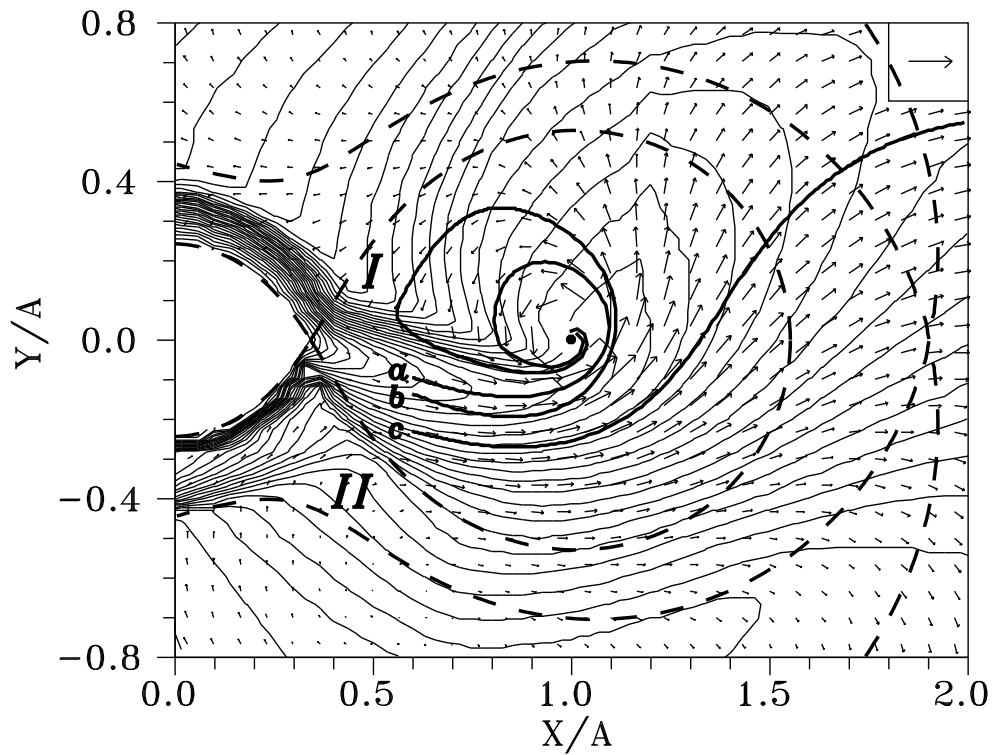


Fig. 7.— Same as Figure 1 for calculation 7 from Table I.

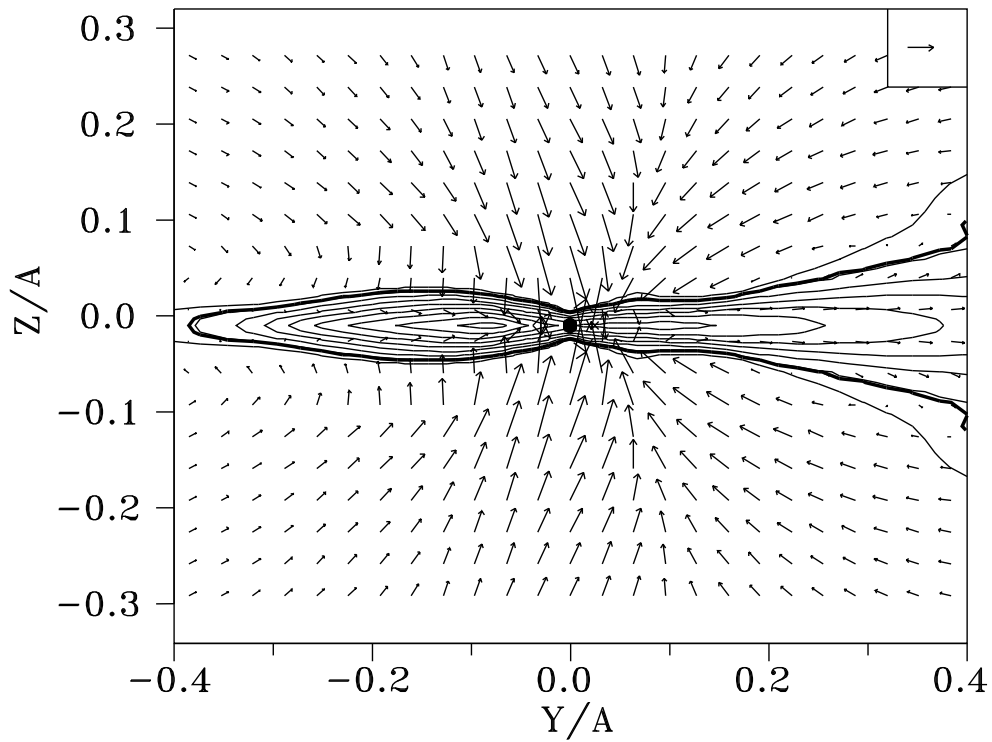
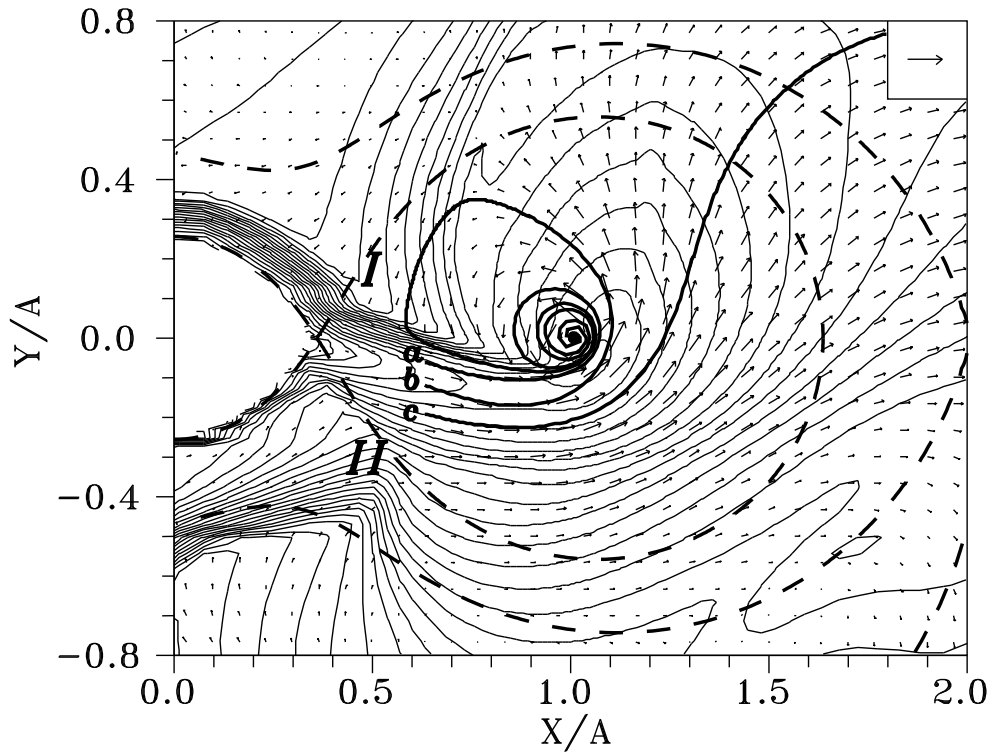


Fig. 8.— Same as Figure 1 for calculation 8 from Table I.

interacts with the matter flowing from the surface of the donor star, and substantially changes the mass exchange regime in the system [23, 25]. Another part of the circumbinary envelope (flowline ‘*b*’) passes around the accretor and undergoes a shock interaction with the edge of the jet facing the direction of the orbital motion. This interaction leads to the absence of a shock interaction of the stream flowing from L_1 with the gas of the forming disk. The stream, deflected by the envelope gas, comes at the disk along a tangent, and does not produce a shock disturbance at the disk edge (“hot spot”). At the same time, the interaction of the stream with the circumbinary envelope results in the formation of an extended shock wave (denoted *I* in the figures) along the edge of the stream, which can be considered equivalent to a “hot spot” on the disk in terms of its observational manifestation [22, 24]. The interaction of the circumbinary envelope with the material in the stream also leads to the formation of shock wave *II*.

The flow pattern undergoes qualitative changes in calculations with the higher index $\gamma = 1.2$ (Figures 1 and 3). This is revealed primarily in the absence of the accretion disk. Analysis of the flowlines presented in Figures 1a and 3a shows that some portion of the stream material (flowline ‘*a*’) flows directly onto the accretor, whereas another portion (flowline ‘*b*’) passes around the accretor and undergoes a shock interaction with the stream flowing from L_1 , without forming a disk. This fact is supported by the appearance of the density and velocity-vector fields in the YZ plane in Figures 1b and 3b. Comparison of these with Figures 2b and 4b provides conclusive evidence for the absence of an accretion disk for the higher γ value. Note that this result is in agreement with [14, 16], which demonstrated that a disk forms only when γ is close to unity ($\gamma < 1.1$). Additional distinctions in the flow pattern for the different γ reveal themselves in changes of the directions of flows in the system. In particular, analysis of the gas motions in the Z direction shows that, for the higher γ , the gas moves predominantly away from the equatorial plane (Figures 1b and 3b), whereas for $\gamma \sim 1$, it moves from higher heights toward the accretion disk (Figures 2b and 4b).

Along with the qualitative differences in the flow pattern, the variations in the value of γ give rise to significant quantitative changes. In particular, for the low value of γ , the influence of the circumbinary envelope on the surface of the donor star substantially

increases. This leads to an increase in the rate of mass loss by the donor star and, as a consequence, to an increase in the matter accretion rate by a factor of 1.5–2.

3.2. The effect of \mathcal{M}

Pairs of calculations that can be used to assess the role of \mathcal{M} are denoted in Table I by the numbers 4, 5 and 6, 7. To study the role of the parameter \mathcal{M} , we compared calculations in which the gas velocity at the near-surface layer of the donor star was taken to be small (the Mach number $\mathcal{M} = 0.08$ in calculation 4 and the Mach number $\mathcal{M} = 0$ in calculation 6) with calculations in which the gas velocity component normal to the surface was equal to the local sound speed ($\mathcal{M} = 1$ for models 5 and 7 in Table I).

The results indicate that a number of minor quantitative changes arise in the flow pattern. In particular, as the Mach number increases, we observe a growth in the rate of mass loss by the donor star due to the “stripping” of its stellar atmosphere by the envelope gas. This effect is quite natural, since an increase in the near-surface gas velocity is accompanied by an increase in the overall extent of the atmosphere, which leads to more intense stripping of atmospheric material by the gas of the circumbinary envelope. Note, however, that the growth of the mass-loss rate of the donor star does not influence the accretion rate, which remains virtually constant as the Mach number varies.

At the same time, the general flow pattern retains all the previously determined qualitative characteristics (see Figures 4 and 5 and also Figures 6 and 7). Moreover, the basic parameters of the gas flows, dimensions and position of the accretion disk, and position and intensity of shock waves *I* and *II* remain virtually unchanged. This, in turn, suggests that \mathcal{M} only weakly influences the flow structure.

3.3. The effect of ϵ

The parameter $\epsilon = c_1/(\Omega A)$ was first introduced by Lubow and Shu [26], and was used as a small parameter. Let us estimate the characteristic range of this parameter for various types of binary systems. Combining the expressions $\Omega A = \sqrt{GM/A}$ and $c_1 = \sqrt{\gamma RT_1}$, we can represent ϵ as

$$\epsilon = 0.003 T_1^{1/2} P^{1/3} M_{M_\odot}^{-1/3} \gamma^{1/2} .$$

Here, the orbital period P is expressed in years and the total mass M of the system in solar masses M_\odot .

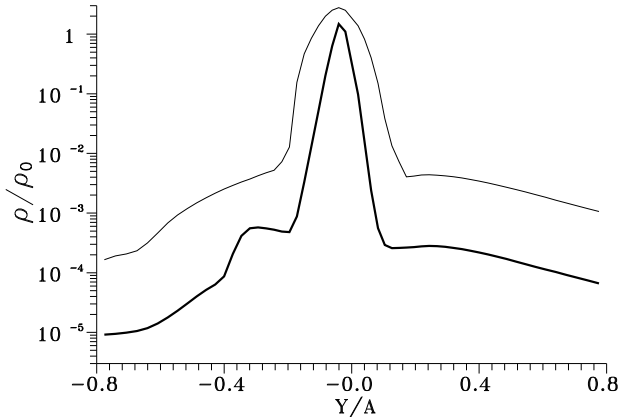


Fig. 9.— One-dimensional density profiles for calculations 2 and 4 specified in Table I. The density values are taken along the straight line in the equatorial plane and passing through the point $0.6A$ perpendicular to the line connecting the centers of the components of the system.

Let us assume that the gas temperature at the donor star is 10^4K . The range of ϵ values characteristic of this case is presented in Table II for various P and M . Analysis of the data in Table II shows that the range of ϵ is rather small ($\sim 0.001 \div 0.3$). However, ϵ cannot always be considered a small parameter.

Table II.

$M = M_\odot$		$M = 10M_\odot$		$M = 100M_\odot$	
P	ϵ	P	ϵ	P	ϵ
year	0.3	year	0.13	year	0.065
month	0.13	month	0.05	month	0.028
day	0.04	day	0.02	day	0.009
hour	0.014	hour	0.006	hour	0.003
minute	0.0037	minute	0.0017	minute	0.0008

To determine the effect of the parameter ϵ , we compare calculations 2 and 4, and 7 and 8. In the first pair of calculations, we varied ϵ from 0.15 to 0.016, and in the second pair, from 0.016 to 0.04. Analysis of the results (Figures 2, 4, 7, and 8) shows that the qualitative flow pattern remains unchanged for various ϵ : an accretion disk forms in the system; there is no "hot spot" in the region of interaction of the stream with the disk; the directions of the flows coincide; and the forming circumbinary envelope interacts

with the stream, producing the shock waves *I* and *II*. In addition, a number of quantitative changes are observed as ϵ is increased. In particular, the cross section of the stream increases in the calculations with the larger ϵ . This is supported by Figure 9, which presents one-dimensional density profiles for calculations 2 and 4. The density values are taken along the straight line in the equatorial plane passing through the point $0.6A$ perpendicular to the line connecting the centers of the system's components. This conclusion is consistent with the results of Lubow and Shu [26], who showed that, for small ϵ , the width of the stream is ϵ . In addition to the increase in the stream size for the larger value of ϵ , we note an increase of the disk thickness and the accretion rate.

3.4. The effect of q

In this study, we examined systems in which the parameter $q = M_2/M_1$ takes on only two values: $q = 1$ in calculations 1–5 and $q = 5$ in calculations 6–8. Assessment of the role of this parameter can be made using calculations 5 and 7, in which all parameters except q were the same. Comparison of the results presented in Figures 5 and 7 shows that the qualitative flow pattern remains unchanged, although some quantitative variations are present. This indicates that the calculation results depend only slightly on the adopted ratio of the masses of the components when $q \geq 1$.

The dependence of the flow pattern on q when $q < 1$ requires additional study. According to [27, 28], when $q < 1$, the flow pattern undergoes significant changes, which is reflected, in particular, in clear observational manifestations. In addition, considerable tidal disturbances are possible when the mass of the donor star is large. A detailed study of the influence of the parameter q will be presented in a future paper.

4. Conclusion

Analysis of the 3D gas-dynamical calculations performed here enables us to sort the parameters of the problem according to their influence on the flow pattern in a semidetached binary system. The variation in the adiabatic index γ has the largest effect on the solution. The influence of \mathcal{M} and ϵ on the flow pattern is small, and leads only to unimportant quantitative variations of the solutions without changing the overall qualitative flow pattern. The ratio q of the

masses of the two components also does not exert a significant influence for the region $q \geq 1$.

Since qualitative changes of the flow pattern depend only on the adopted value of the parameter γ , let us consider the mechanism of its action upon the flow and summarize the main features of the gas-flow structure that should be observed in semidetached binaries. We considered the flow of a nonviscous, non-heat-conducting gas in a binary system without magnetic and radiation fields. In the model, the assumption that the gas is ideal formally implies neglect of radiative losses, although small values of the adiabatic index γ imitate energy losses in the system (see, for example, [3]). In particular, when $\gamma \sim 1$, a solution close to the isothermic solution is realized [28]. In the above calculations, we used the two γ values 1.2 and 1.01, and, thus, obtained solutions corresponding to models with different energy-loss rates. The flow patterns calculated in these two cases display fundamental differences. For example, in the calculations performed with $\gamma = 1.2$, the accretion disk does not form at all. The increase in energy losses in the system in the calculations for the close to isothermal case ($\gamma \sim 1$) leads to the formation of an accretion disk and a corresponding change in the accretion mechanism.

In typical binaries, the gas between the components is ionized, and the corresponding energy-loss mechanisms work efficiently, so the real flow pattern should be described by a close to isothermal model [30, 31]. As we noted above, in this case, the flow pattern is characterized by the following features: the stream of gas flowing from L_1 forms both an accretion disk and a circumbinary envelope in the system. Further, the envelope gas exerts a considerable influence on the structure of gas flows in the system [23–25]. In particular, the envelope gas interacts with the stream of matter flowing from the vicinity of L_1 and deviates it, giving rise to a shockless (tangential) interaction of the stream with the outer edge of the forming accretion disk and, therefore, to the absence of a "hot spot" in the disk. At the same time, the interaction of the envelope gas with the stream is responsible for the formation of an extended shock wave at the edge of the stream, whose observational manifestations can be considered equivalent to those of a hot spot in the disk [24].

This work was supported by the Russian Foundation for Basic Research (project code 96-02-16140), the State Scientific and Technological Program "As-

tronomy" ("Computational Astrophysics" Section), and the "Cosmion" Scientific Educational Center for Cosmoparticle Physics.

REFERENCES

- [1] Prendergast, K. H., 1960, ApJ, 132, 162
- [2] Sawada, K., Matsuda, T., Hachisu, I., 1986, MNRAS, 219, 75
- [3] Sawada, K., Matsuda, T., Inoue, M., Hachisu, I., 1987, MNRAS, 224, 307
- [4] Spruit, H. C., Matsuda, T., Inoue, M., Sawada, K., 1987, MNRAS, 229, 517
- [5] Różyczka, M., Spruit, H. C., 1989, in Meyer F., Duschl W., Frank J., Meyer-Hofmeister E., eds, Theory of accretion disks, Kluwer, Dordrecht, p. 341
- [6] Taam, R. E., Fu, A., Fryxell, B. A., 1991, ApJ, 371, 696
- [7] Blondin, J. M., Richards, M. T., Malinowski, M. L., 1995, ApJ, 445, 939
- [8] Murray, J. R., 1996, MNRAS, 279, 402
- [9] Boyarchuk, A. A., Bisikalo, D. V., Kuznetsov, O. A., Chechetkin, V. M., 1997, in Mashevitch A. G., ed., Binary Stars, Kosmosinform, Moscow, p. 18 (in Russian)
- [10] Fridman, A. M., Khoruzhii, O. V., 1994, in Gor'kavii N. N., Fridman A. M. Physics of planetary rings, Moscow, Nauka, p. 282 (in russian)
- [11] Bisikalo, D. V., Boyarchuk, A. A., Chechetkin, V. M., Kuznetsov, O. A., Molteni, D., 1998, in preparation
- [12] Nagasawa, M., Matsuda, T., Kuwahara, K., 1991, Numer. Astroph. in Japan, 2, 27
- [13] Hirose, M., Osaki, Y., Minishige, S., 1991, PASJ, 43, 809
- [14] Molteni, D., Belvedere, G., Lanzafame, G., 1991, MNRAS, 249, 748
- [15] Sawada, K., Matsuda, T., 1992, MNRAS, 255, 17
- [16] Lanzafame, G., Belvedere, G., Molteni, D., 1992, MNRAS, 258, 152
- [17] Belvedere, G., Lanzafame, G., Molteni, D., 1993, A&A, 280, 525
- [18] Lanzafame, G., Belvedere, G., Molteni, D., 1994, MNRAS, 267, 312

- [19] Meglicki, Z., Wickramasinghe, D., Bicknell, G.V., 1993, MNRAS, 264, 691
- [20] Armitage, P. J., Livio, M., 1996, ApJ, 470, 1024
- [21] Armitage, P. J., Livio, M., 1998, ApJ, 493, 898
- [22] Bisikalo, D. V., Boyarchuk, A. A., Kuznetsov, O. A., Chechetkin, V. M., 1997, Astron. Reports, 41, 786, preprint astro-ph/9802004
- [23] Bisikalo, D. V., Boyarchuk, A. A., Kuznetsov, O. A., Chechetkin, V. M., 1997, Astron. Reports, 41, 794, preprint astro-ph/9802039
- [24] Bisikalo, D. V., Boyarchuk, A. A., Kuznetsov, O. A., Khruzina, T. S., Cherepashchuk, A. M., Chechetkin, V. M., 1998, Astron. Reports, 42, 33, preprint astro-ph/9802134
- [25] Bisikalo, D. V., Boyarchuk, A. A., Chechetkin, V. M., Kuznetsov, O. A., Molteni, D., 1998, MNRAS, in press, preprint astro-ph/9805261
- [26] Lubow, S. H., Shu, F. H., 1975, ApJ, 198, 383
- [27] DiStefano, B., Nelson, L. A., 1996, in Greiner J., ed., Supersoft X-Ray Sources, Springer, Berlin
- [28] King, A. R., Frank, J., Kolb, U., Ritter, H., 1997, ApJ, 484, 844
- [29] Landau, L. D., Lifshiz, E. M., 1959, Fluid Mechanics. Pergamon, Elmsford
- [30] Bisikalo, D. V., Boyarchuk, A. A., Kuznetsov, O. A., Chechetkin, V. M., 1996, Astron. Reports, 40, 653
- [31] Bisikalo, D. V., Boyarchuk, A. A., Kuznetsov, O. A., Chechetkin, V. M., 1996, Astron. Reports, 40, 662